Pre-Steady-State and Steady-State Kinetic Studies on Transcription Initiation Catalyzed by T7 RNA Polymerase and Its Active-Site Mutants K631R and Y639F†

A-Young Moon Woody,*,‡ Patricia A. Osumi-Davis,‡ Meenaxi M. Hiremath,§ and Robert W. Woody‡

Department of Biochemistry and Molecular Biology, Colorado State University, Fort Collins, Colorado 80523, and Department of Microbiology and Immunology, University of North Carolina, Chapel Hill, North Carolina 27599

Received March 13, 1998; Revised Manuscript Received September 14, 1998

ABSTRACT: The kinetic mechanism of transcription initiation was studied under conditions that allow a single nucleotide addition to an initiating dinucleotide without interference of enzyme−DNA dissociation or protein recycling. Pre-steady-state kinetic studies have provided polymerization rate constants of 3.9, 5.9, and 3.9 s^{-1}, reverse polymerization rate constants of 3.2, 2.1, and 2.8 s^{-1}, and dissociation constants for the incoming nucleotide of 26, 49, and 24 μM at 21 °C, respectively, for the wild type and its active-site mutants K631R and Y639F. The results suggest a model in which K631 interacts with the phosphate group(s) of the incoming substrate. The internal equilibrium constants for the bound species are close to unity, consistent with the values for other phosphoryl transfer enzymes. The rate constants for chemical bond formation are at least 50 times higher than the rate constants for product dissociation. The product release rate constants, k_3, are comparable to the steady-state rates, suggesting that the rate-determining step for all three enzymes may be a product dissociation step. The existence of two possible conformers E and E′ that are in rapid equilibrium is postulated, to reconcile reduced burst sizes with full activity of the mutant enzymes. Both forms can form the quaternary complex, but only the E form is capable of catalyzing phosphodiester bond formation. The fraction of the catalytically active E form varies from essentially 100% for the wild type to 38 and 32% for the mutants K631R and Y639F, respectively. Upon entering the elongation phase, the E form becomes the dominant form in all three enzymes, leading to comparable rates of elongation for the wild type and Y639F mutant. The rate of synthesis of long transcripts is markedly diminished for the K631R mutant due to decreased processivity.

Elucidation of the mechanism of RNA polymerase-catalyzed RNA synthesis will greatly aid our understanding of gene expression. Transcription initiation is the first phase in the transcription process and plays a major role in gene expression. The RNA polymerase from T7 bacteriophage is an ideal model enzyme for mechanistic studies on many aspects of the transcription process because it is a single-subunit enzyme (99 kDa) capable of RNA synthesis without involving additional factors and can be overproduced (*1*). One amino acid, Asn748, has been identified as a determinant for the promoter specificity (*2*), and groups in the promoter that are significant in the enzyme−promoter interaction have been identified (*3*). Several catalytically essential and significant functional amino acids (D537, K631, Y639, D811, and D812) (*4*−*7*) have been identified through site-directed mutagenesis, and the four C-terminal residues ($FAFA^{883}$) (*8*) through cassette mutagenesis. The crystal structure of the enzyme at 3.3 Å resolution (*9*) has shown the locations of the important functional groups in the putative DNA-binding region. Characterization of the identified amino acids at the transcription initiation level was possible by steady-state kinetic studies on the wild-type and mutant enzymes (*4*, *5*, *8*) using small synthetic oligonucleotide templates containing the T7 promoter (*10*). Two conserved and essential Asp residues, D537 and D812, act as metal-binding ligands by bridging the two metal ions with their monodentate carboxylate oxygens (*11*), suggesting that T7 RNA polymerase catalyzes RNA synthesis via a metal ion-dependent mechanism analogous to that proposed for DNA polymerase I (*12*). Studies on mutants D537N, D537E, D812N, and D812E suggest that the geometry of the metal binding may be crucial in catalytic competence (*11*). The catalytically significant Y639 is reported to distinguish the 2′-ribose group via H-bonding (*13*).

Pre-steady-state kinetic measurements allow individual steps in the reaction pathway to be determined. The active-site mutants may display characteristics in the reaction steps different from those of the wild type, thus permitting us to gain information on the involvement of a particular amino acid. Pre-steady-state kinetic studies on the wild-type enzyme−DNA interaction (*14*, *15*) and transcription initiation by the wild-type enzyme (*16*, *17*) have been reported. In this paper, we present pre-steady-state kinetic parameters on the addition of a single nucleotide to an initiating dinucleotide catalyzed by the wild-type and the mutant K631R and Y639F enzymes and discuss the implications of the results.

† Supported by NIH Grant GM-23697 (A-Y.M.W. and R.W.W.). M.M.H. was an REU (Research Experience for Undergraduates) student supported by NSF (DBI-9531511).

* To whom correspondence should be addressed.

‡ Colorado State University.

§ University of North Carolina.

[1] Abbreviations: PP_i, pyrophosphate; buffer A, 10 mM Tris-HCl (pH 7.9) containing 50 mM KCl, 10 mM $MgCl_2$, and 1 mM DTT.

10.1021/bi9805801 CCC: $15.00
Published on Web 10/23/1998

EXPERIMENTAL PROCEDURES

For all the kinetic studies, buffer A[1] was used. Buffers, glass-distilled water, and 0.15 M EDTA were thoroughly degassed before being used.

The methodology for producing the mutant enzymes has been described previously (*4*). The purification of the wild-type and the mutant enzymes was based on published procedures (*18*).

Enzyme activity was determined by the DE81 filter-binding method (*19*). Assay solutions contained 100 nM T7 RNA polymerase, 50 nM pT713 DNA (supercoiled), 400 μM to 3 mM GTP, 400 μM ATP and CTP, and 400−800 μM UTP, including 0.5 μCi of [^{3}H]UTP in buffer A, and the reaction was carried out for 5 min at 37 °C. Enzyme activities were 4.9×10^5, 7.3×10^4, and 3.9×10^5 units for the wild-type and the mutant K631R and Y639F enzymes, respectively. One unit of specific activity was defined as 1 nmol of UMP incorporated per milligram of enzyme per hour at 37 °C under our assay conditions. The purity of the enzyme was evaluated using SDS−PAGE, and our enzyme is typically greater than 95% pure. Concentrations of enzyme solutions for the kinetic measurements were determined spectroscopically using a molar extinction coefficent of 1.4×10^5 M^{-1} cm^{-1} (*20*).

Two oligonucleotide templates containing the T7 promoter were used. They were synthesized and their purities checked by HPLC (Ransom Hill, Ramona, CA). Absorption spectra were measured and concentrations were calculated on the basis of the extinction coefficients of the templates calculated from the formula given in the published literature (*21*).

For pre-steady-state kinetic parameters, template A was used.

Template A: 5'-TAATACGACTCACTATA*GGACT*-3'

3'-ATTATGCTGAGTGATAT*CCTGA*-5'

For the template challenge method, template B was used.

Template B: 5'-TAATACGACTCACTATA*GGCTA*-3'

3'-ATTATGCTGAGTGATAT*CCGAT*-5'

Nucleotides were of the purest quality from Pharmacia (Piscataway, NJ). GpG and all other chemicals were from Sigma Chemicals (St. Louis, MO). [α-^{32}P]ATP was purchased from ICN Pharmaceuticals (Costa Mesa, CA).

For the template challenge method, the reaction mixture contained 10 nM wild-type enzyme (or mutant K631R or Y639F), 200 nM template A, 200 μM GpG, and 100 μM ATP (and 1 mM template B where applicable) in buffer A at 21 °C. The product GpGpA was fractionated by 25% urea−PAGE and analyzed on a PhosphorImager SP (Molecular Dynamics, Sunnyvale, CA).

For pre-steady-state kinetics, a quench-flow system (Biologic SFM-3F/Q; Molecular Kinetics, Inc., Pullman, WA) that allows measurements of rates in the millisecond range was used for reactions up to 2 s, and a manual method was used to extend the time from 5 to 15 s. In the rapid-mixing module, a programmed step motor is used to drive the reactants in two separate syringes into a rapid-mixing chamber, and then through a delay line into a quenching solution.

One syringe contained 200 nM polymerase, 400 nM 22 bp oligonucleotide template (template A), and 400 μM GpG in buffer A, and the other syringe contained ATP at concentrations ranging from 10 to 200 μM, including varying amounts of [α-^{32}P]ATP, and 20 mM $MgCl_2$ in buffer A. In the final reaction, the concentration of each reactant becomes half of the concentration in each syringe. After the reaction was quenched with 0.15 M EDTA (this concentration was sufficient to quench the reaction under our experimental conditions), the product GpGpA was fractionated by 25% urea−PAGE and quantitated on a PhosphorImager SP. All the experiments were performed at 21 °C. For each reaction progress curve, three to five independent experiments were performed. To make sure that the order of component addition did not make a difference, the following experiments were performed for the three enzyme systems; one syringe contained enzyme, template A, GpG, and ATP, and the other syringe contained Mg^{2+} under the identical conditions described above. It was found that there was no difference in kinetic parameters obtained under the two different conditions.

The conditions of steady-state kinetics and the subsequent treatment of the products were the same as in the pre-steady-state kinetics experiments, except that the final enzyme concentration was 5 nM.

Kinetic data were fit to eqs 1 and 2 (see below) by the nonlinear least-squares method using the program Axum (TriMetrix, Seattle, WA) which is based on the Marquardt−Levenberg nonlinear least-squares algorithm (*22*). The errors given in Tables 2 and 3 are standard errors, unless otherwise stated. The 68% confidence interval is ±one standard error for a single parameter (*22*).

RESULTS

Pre-steady-state kinetics allow determination of individual steps in the reaction pathway, and we have examined the kinetic pathway describing a single nucleotide addition to a dinucleotide initiator catalyzed by the wild-type and the mutant K631R and Y639F enzymes.

A minimal working scheme is presented in Scheme 1

Scheme 1

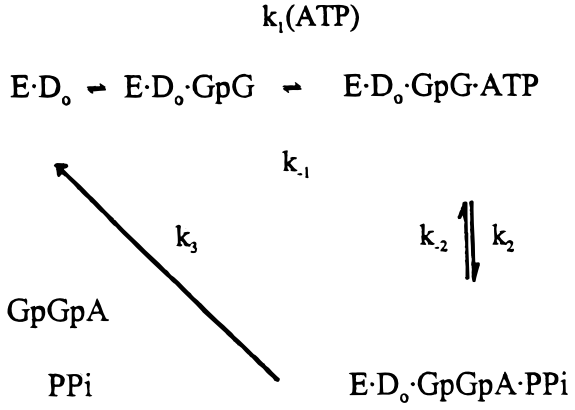

where E represents enzyme, D a template (template A), GpG an initiating dinucleotide, and GpGpA the trinucleotide

Table 1: Stability of the Enzyme−Template A Complex during the Synthesis of GpGpA on Template at 21 °C[a,b]

	[GpGpA] (nM)					
	wild type		K631R		Y639F	
time (s)	A	B	A	B	A	B
10	5.8 ± 1.1	6.0 ± 1.0	3.1 ± 1.1	3.1 ± 1.1	3.8 ± 1.7	4.1 ± 0.3
15	8.5 ± 1.2	8.2 ± 0.6	4.8 ± 1.0	4.1 ± 1.1	5.1 ± 3.1	5.2 ± 1.1
20	9.7 ± 1.0	10.7 ± 1.4	5.8 ± 2.0	5.4 ± 1.8	6.8 ± 4.4	5.1 ± 0.6
25	11.6 ± 2.6	10.4 ± 2.0	6.3 ± 1.8	5.4 ± 3.0	5.9 ± 3.4	5.9 ± 1.4
30	13.0 ± 1.4	11.7 ± 2.8	7.0 ± 1.9	6.7 ± 1.4	6.6 ± 1.9	5.9 ± 1.5
45	18.8 ± 1.9	15.6 ± 5.6	11.3 ± 3.0	8.2 ± 2.9	9.8 ± 4.5	7.0 ± 0.3
60	26.9 ± 3.6	17.6 ± 5.4	12.8 ± 4.7	9.4 ± 4.9	10.2 ± 3.3	8.1 ± 0.9
120	64.0 ± 9.9	39.0 ± 8.3	29.0 ± 10.2	15.8 ± 6.7	24.4 ± 8.2	16.4 ± 5.7

[a] These values are the average of three to five independent experiments. [b] The reaction conditions are described in Experimental Procedures. For A, the wild-type enzyme (or K631R or Y639F), template A, and GpG were preincubated for 5 min before ATP was added to start the reaction. For B, the wild-type enzyme (or K631R or Y639F), template A, and GpG were preincubated for 5 min before ATP and template B were added to start the reaction.

product. $E{\cdot}D_o$ is the open complex of RNA polymerase with the template. The following experimental conditions were used so that only steps 1−3 in Scheme 1 were relevant, and the enzymatic reaction becomes analogous to $E + S \rightleftarrows ES \rightleftarrows EP \rightarrow E + P$. The transient kinetic formulation for this enzymatic mechanism is well established in the literature (*23*−*26*).

(a) The ternary complex, $E{\cdot}D_o{\cdot}GpG$, was derived by incubating enzyme, template A, and GpG prior to the addition of the nucleotide−Mg^{2+} complex. (b) A template concentration of 200 nM was used throughout our experiments. The $(K_m)_{app}$ values for the promoter binding are 13, 23, and 6 nM, respectively, for the wild type, Y639F (*4*), and K631R (*5*). The K_d values for the wild type using the oligonucleotide template is reported to be 3.6 nM at 25 °C (*14*). (c) A saturating concentration of GpG (200 μM) was used. The rate of synthesis of GpGpA did not change when the GpG concentration was varied from 200 to 800 μM (data not shown). (d) The enzyme−template A complex remained stable up to 20−30 s during the time of the product GpGpA synthesis as determined by the template challenge method (Table 1). (e) Release of the products is assumed to be irreversible. (f) A possible enzyme conformational change taking place at each relevant step will not be considered here.

Enzyme−Template A Complexes Remain Stable during the Time of Pre-Steady-State Kinetic Measurements. We had to make sure that the enzyme−template A complexes remain stable during the time of the pre-steady-state kinetic measurements on the synthesis of GpGpA on template A. This was tested using the template challenge method. It was found that for up to 20−30 s, the enzyme−template A complex remains stable during the time of GpGpA synthesis. It was found that the rate of GpGpA formation was the same whether the reaction was initiated with $E{\cdot}D_o{\cdot}GpG$ and ATP or $E{\cdot}D_o$, GpG, and ATP at saturating template A and GpG concentrations. We have used template B, which does not lead to ATP incorporation, to challenge template A so that the level of production of GpGpA will decrease once template B takes the place of template A. The results are given in Table 1.

Steady-State Kinetics. Prior to the characterization of pre-steady-state kinetics for the wild type and the mutants K631R and Y639F, steady-state kinetic parameters for the synthesis of GpGpA were obtained using 5 nM enzyme, 200 nM template A, 200 μM GpG, and 100−200 μM ATP under the same conditions used for the pre-steady-state experiments. The $(k_{cat})_{app}$ values obtained are 0.031 ± 0.010, 0.019 ± 0.006, and 0.023 ± 0.005 s^{-1}, respectively, at 21 °C for the wild type and the mutants K631R and Y639F.

Pre-Steady-State Kinetics. The pre-steady-state kinetic experiments on the addition of a single nucleotide (ATP and [α-^{32}P]ATP) to the initiating dinucleotide GpG have been performed using the wild-type enzyme and the mutants K631R and Y639F. Figure 1 shows a gel pattern of the time-dependent appearance of the product GpG·[α-^{32}P]A bands catalyzed by the wild-type enzyme at 21 °C. By quantitating the gel bands and the control band of radioactive ATP, we calculated the concentrations of GpGpA at various times.

Panels A−C of Figure 2 are the pre-steady-state kinetic progress curves of GpGpA appearance at 21 °C, using ATP concentrations of 100, 200, and 100 μM, respectively, representing the wild type and the mutants K631R and Y639F. The results indicate biphasic progress curves that can be described by an exponential followed by a linear phase:

$$P = A[1 - \exp(-k_{obs}t)] + mt \qquad (1)$$

The reaction progress curves shown in Figure 2 were fit to eq 1 by a nonlinear least-squares method as described in Experimental Procedures to obtain the burst amplitude A, the observed rate constant k_{obs}, and the slope m. These values are listed in Table 2. The burst rate is much faster than the steady-state rate, indicating that k_2 is much larger than k_3. The biphasic progress curves indicate that the rate-limiting step is a step other than the chemical step for the wild type and the mutants K631R and Y639F.

The rate constants obtained for the linear phase by the pre-steady-state kinetic method (k_{cat} = 0.023 ± 0.004, 0.010 ± 0.002, and 0.012 ± 0.002 s^{-1} for the wild type and the mutants K631R and Y639F, respectively) are compared to the values obtained by steady-state kinetic analysis (k_{cat} = 0.031 ± 0.010, 0.019 ± 0.006, and 0.023 ± 0.006 s^{-1}, respectively). The rate constants obtained by the two methods agree barely within experimental error, but they are comparable. Therefore, the linear phase was assumed to represent the steady-state phase of the enzymatic reaction.

The burst amplitude should be close to the active enzyme concentration if the reverse polymerization rate constants k_{-2} and product release rate constant k_3 in Scheme 1 are

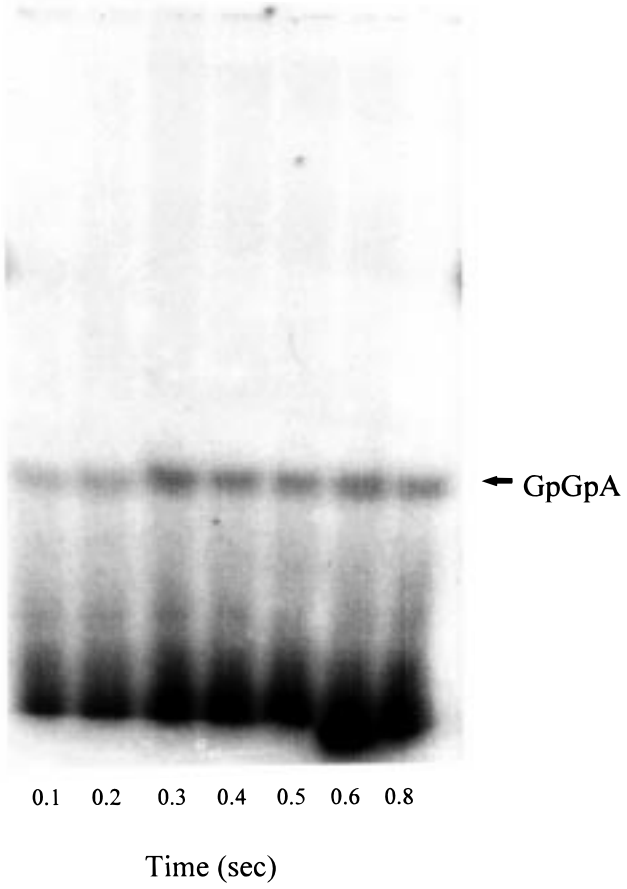

FIGURE 1: Gel electrophoresis pattern of GpGpA production at varying times. The reaction was performed at 21 °C, and the reaction mixture contained 100 nM wild-type T7 RNA polymerase, 200 nM template A, 200 μM GpG, and 100 μM ATP in buffer A. After the reaction was quenched with 0.15 M EDTA, the product GpGpA was fractionated by 25% urea−PAGE.

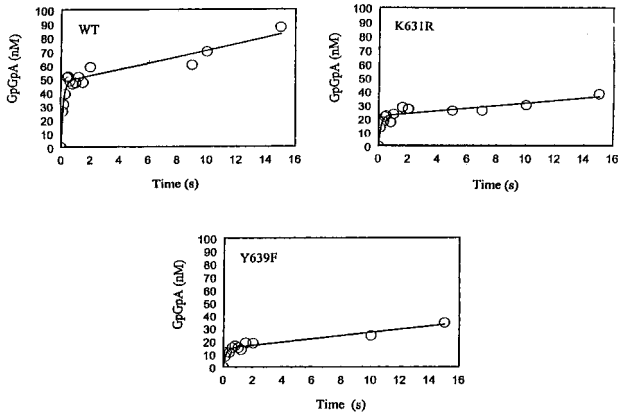

FIGURE 2: Pre-steady-state kinetic reaction profiles of the incorporation of ATP into GpGpA. The reaction conditions were the same as those described in Figure 1. The product GpGpA was quantitated on a PhosphorImager.

insignificant (*26*). The burst amplitudes shown here are about 48, 22, and 14% of the spectroscopically determined enzyme concentration, respectively, for the wild type and the mutants K631R and Y639F. These results imply that either the rate constants k_{-2} and/or k_3 may not be negligible or the concentration of active enzyme species may be smaller than the spectroscopically determined enzyme concentration. Therefore, we have included k_{-2} and k_3 in our kinetic

Table 2: Parameters Obtained from Pre-Steady-State Kinetic Progress Curves[a]

enzyme	[ATP] (μM)	A (nM)	k_{obs} (s^{-1})	m (nM s^{-1})
wild type	100	47.5 ± 2.2	6.1 ± 1.3	2.3 ± 0.3
K631R	200	22.0 ± 1.4	6.6 ± 2.2	1.0 ± 0.2
Y639F	100	14.3 ± 0.9	6.0 ± 1.7	1.2 ± 0.1

[a] Experimental conditions and data analysis are described in Experimental Procedures.

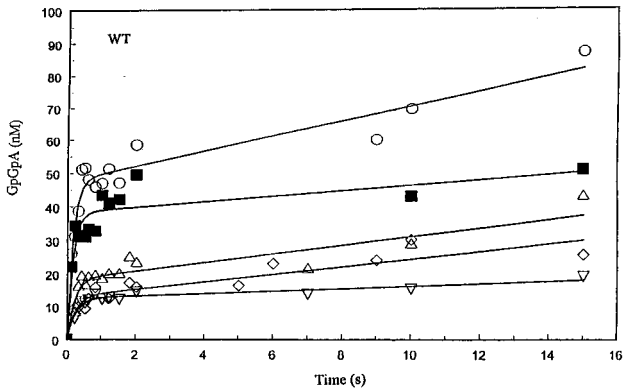

FIGURE 3: ATP concentration-dependent pre-steady-state reaction profile of GpGpA synthesis by the wild-type enzyme. The reaction conditions and the product treatment were the same as those described in Figures 1 and 2 except that ATP concentrations were varied as follows: 100 (○), 50 (■), 25 (△), 10 (◇), and 5 μM (▽).

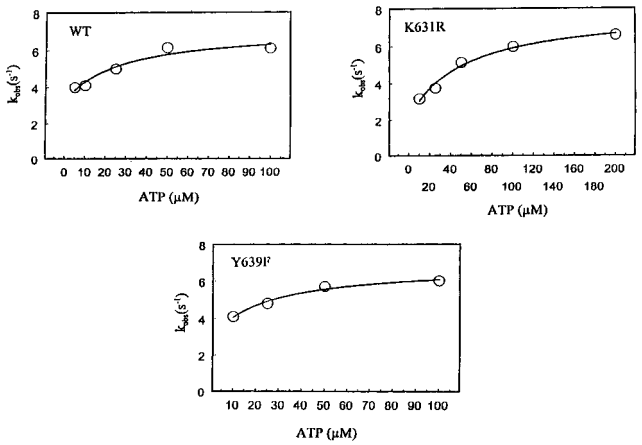

FIGURE 4: ATP concentration-dependent variation of the rate constants (k_{obs}) obtained from the burst phase of the reaction profiles of the wild-type and mutant K631R and Y639F enzymes. The reaction conditions and data treatment were the same as those described in Figures 1 and 2.

formulation. Since no known inhibitor is available to completely block reinitiation of RNA synthesis (*27*, *28*) by T7 RNA polymerase to assess active enzyme concentrations, we have handled this problem by using the same batch of enzyme throughout our pre-steady-state kinetic experiments and have examined enzyme activity regularly during this period. The enzymatic activities of the wild type and the mutant Y639F and K631R enzymes obtained on template pT713 supercoiled DNA have remained the same within experimental error throughout the pre-steady-state kinetic studies. All these enzymatic activities are comparable to the published values (*5*). Therefore, our enzymes are assumed to be 100% active in our data analysis.

The pre-steady-state progress curves measured at ATP concentrations of 5, 10, 25, 50, 100, and 200 μM were fit to

Table 3: Kinetic Constants Obtained for the Addition of ATP to GpG at 21 °C[a]

enzyme	k_2 (s^{-1})	k_{-2} (s^{-1})	k_3 (s^{-1})[b]	K_{d1} (μM)	K_{int}[c]
wild type	3.9 ± 0.7	3.2 ± 0.8	0.05 ± 0.01	25.5 ± 27.0	1.2 + 0.7/−0.4
K631R	5.7 ± 0.5	2.1 ± 0.6	0.05 ± 0.01	49.3 ± 23.8	2.8 + 1.3/−0.9
Y639F	3.9 ± 0.6	2.8 ± 0.9	0.08 + 0.01/−0.02	23.8 ± 20.8	1.4 + 1.0/−0.5

[a] Experimental conditions and data analysis are described in Experimental Procedures. [b] k_3 ($=m/A$) was calculated from the mean values of m and A. Errors were estimated by including the standard errors in m and A to give maximal and minimal values of k_3. The resulting deviations from the mean are shown as plus or minus. [c] K_{int} ($=k_2/k_{-2}$) and errors were estimated by the same method used for k_3, described in footnote b.

Table 4: Comparison of the Burst Amplitudes and the A_0 Values Calculated from the Rate Constants[a]

enzyme	$(A_0)_{exp}$	$(A_0)_r$	$(A_0)_{calc}$
wild type	0.48	0.60	0.55
K631R	0.22	0.28	0.73
Y639F	0.14	0.18	0.57

[a] $(A_0)_{exp}$ values are burst amplitudes obtained directly from experiments. $(A_0)_r$ values are revised values based on the new K_{d1} values. $(A_0)_{calc}$ values are obtained from the equation $A_0 = k_2(k_2 + k_{-2})/(k_2 + k_{-2} + k_3)^2$ using the experimentally obtained rate constants (see Table 3).

eq 1 by a nonlinear least-squares method to obtain the parameters k_{obs}, A, and m. Figure 3 shows one example of the plots. The resulting parameters are given in Table 2. The variation of the observed rate constants with ATP concentration is shown in Figure 4 for the wild type and the mutants K631R and Y639F, and these plots indicate consistency with the kinetic pathway shown in Scheme 1. The plot of the rate constant k_{obs} versus the ATP concentration was fit to the hyperbolic equation

$$k_{obs} = (k_2[\mathrm{ATP}])/([\mathrm{ATP}] + K_{d1}) + (k_{-2} + k_3) \quad (2)$$

by a nonlinear least-squares method to obtain k_2 (the rate constant for the polymerization), K_{d1} (the dissociation constant for the nucleotide ATP), and k_{-2} (the rate constant for the reverse polymerization) plus k_3 [the rate constant for the release of the product(s)]. The composite value of k_{-2} and k_3 was evaluated further by using the relationships in eqs 3 and 4 where A is the burst amplitude and m is the slope of the reaction progress curve.

$$A = A_0[\mathrm{E}_0] = k_2(k_2 + k_{-2})[\mathrm{E}_0]/(k_2 + k_{-2} + k_3)^2 \quad (3)$$

$$m = k_{cat}[\mathrm{E}_0] = k_2k_3[\mathrm{E}_0]/(k_2 + k_{-2} + k_3) \quad (4)$$

From eqs 3 and 4, if we assume k_3 is negligible compared to k_2 and k_{-2} in the first approximation, k_3 can be calculated and refined further by iteration. In all cases, the values of k_3 were indeed small compared to k_2 and k_{-2} and iteration was not necessary. The values of k_{-2} were obtained by subtracting the k_3 values from the $k_3 + k_{-2}$ values.

As shown in Table 3, the rate constants k_2 and k_{-2} for the mutant Y639F are the same as the rate constants for the wild-type enzyme within experimental error. On the other hand, the rate constants for the mutant K631R are slightly different from the values for the wild type. The K_{d1} value for the mutant K631R is twice the value for the wild type and the mutant Y639F, suggesting that the K631R mutant binds the incoming nucleotide in the quaternary complex of reactants less strongly than does the wild type. These results suggest an interaction of Lys631 with the phosphate group of the incoming nucleotide. The K_{int} values for the interconversion of the enzyme−substrate complex and the enzyme−product complex (on-enzyme equilibration) were calculated from k_2 and k_{-2} values, and they are close to unity.

The burst amplitudes were reexamined to evaluate the internal consistency of our data and the transient kinetic formulation (Table 4). When the kinetic rate constants k_2, k_{-2}, and k_3 for the wild-type enzyme were substituted into eq 3, an A_0 value of 0.55 was obtained, and this is close to the $(A_0)_r$ value of 0.6, the experimentally determined A_0 value corrected for the fraction of the enzyme that has no bound ATP, calculated from K_{d1}. When a similar analysis was performed for the mutants K631R and Y639F, A_0 values of 0.72 and 0.57 were calculated, which are to be compared with the $(A_0)_r$ values of 0.28 and 0.18. Thus, for the wild-type enzyme, the experimentally obtained burst amplitude is largely due to the on-enzyme equilibration, whereas this explanation alone is not adequate for the mutants K631R and Y639F (see Discussion).

DISCUSSION

This study provides the first pre-steady-state analysis comparing the wild-type T7 RNA polymerase and the active-site mutants K631R and Y639F. The pre-steady-state parameters, k_2, k_{-2}, K_{d1}, and k_3, for a single-nucleotide addition to a dinucleotide initiator on a defined template by these enzymes allowed direct comparison of the fundamental rate parameters of these enzymes.

These results complement earlier steady-state studies of initiation kinetics (tri-, tetra-, and pentanucleotide synthesis) and elongation kinetics (long transcript synthesis) (*4*, *5*).

According to pre-steady-state kinetic analysis, the rate constants for the phosphodiester bond formation step are similar for the wild type and the mutants K631R and Y639F. Thus, the mutations do not seem to significantly affect the intrinsic rate of phosphodiester bond formation.

Steady-state kinetic studies (*5*) gave $(k_{cat})_{app}$ values for the synthesis of trimer from a dinucleotide initiator of 15, 8.3, and 5.4 min^{-1} at 37 °C for the wild type and the mutants K631R and Y639F, respectively. In contrast, for the synthesis of longer transcripts, in which elongation is involved, the $(k_{cat})_{app}$ values for the mutant K631R are nearly one order of magnitude smaller than the value for the wild type, whereas the $(k_{cat})_{app}$ values for the mutant Y639F are similar to the value for the wild type. These differences in the pre-steady-state single-nucleotide addition and steady-state kinetics of short and long transcript synthesis can be reconciled by considering the burst size in the pre-steady-state kinetics.

The reduced burst size for Y639F is especially puzzling in view of the similarity of this mutant to the wild type in the synthesis of long transcripts. We propose that there are

two major enzyme conformers, E and E′, which are in rapid equilibrium. Both forms are able to bind DNA, initiating dinucleotide and NTP to form the quaternary complex, but only form E is able to catalyze phosphodiester bond formation in the initiation complex. In the wild-type enzyme, the equilibrium favors E so that essentially 100% [$(A_0)_r/(A_0)_{cal} = 1.09$] of the enzyme participates in the burst phase of the single-turnover experiment. In the mutants K631R and Y639F, the equilibrium favors E′ so that only 38 [$(A_0)_r/(A_0)_{cal} = 0.38$] and 32% [$(A_0)_r/(A_0)_{cal} = 0.32$], respectively, contribute to the burst phase. If the mutations do not significantly affect the intrinsic rate of phosphodiester bond formation, as our data suggest, the isomerization should lead to a decrease in k_{cat} for steady-state synthesis of trinucleotide by a factor of 2.6 for K631R and of 3.1 for Y639F, relative to that of the wild type. Steady-state measurements of trinucleotide synthesis with initiating GpG on these mutants (*5*) showed k_{cat} values for K631R and for Y639F that are smaller than those for the wild type by factors of 2−3 and 3−4, respectively. On entering the elongation phase, form E becomes the dominant form in Y639F as well as in the wild type. Thus, Y639F has kinetic parameters for long oligonucleotide synthesis that are comparable to those of the wild type. In the case of the K631R mutant, the rate of synthesis of a 60 nt RNA is only about 10% of the rate for the wild type, but this decrease is accompanied by an increase in the rate of abortive product synthesis. The diminished processivity for this mutant makes it difficult to determine the E−E′ equilibrium in the elongation complex for this case, but the total rate of nucleotide incorporation is reduced 2-fold for K631R relative to that of the wild type. Two possibilities could be considered for the defective processivity: (i) the release of PP_i or a conformational change associated with the release of PP_i is blocked or (ii) the release of GpGpA is faster than that of PP_i or the associated conformational change.

The principal effect of Lys → Arg substitution appears to be the destabilization of the Michaelis complex with the incoming nucleotide. Thus, the role of Lys631 seems to be that of interacting with one or more phosphate groups in the incoming nucleotide as it binds and undergoes addition to the primer.

It can be seen that at the level of single-nucleotide addition in the initiation phase, for the three enzymes examined, the k_2 values of chemical bond formation are at least 50 times higher than the k_3 values of product dissociation, and the reverse process of chemical bond formation is not negligible. The internal equilibrium constants, K_{int}, are close to unity for the wild-type and mutant enzymes (Table 3), which is consistent with the K_{int} values observed in phosphoryl group transfer reactions (*23*, *24*, *29*, *30*). The product release rate constants, k_3, are comparable to the steady-state rates, suggesting that the rate-determining step for all three enzymes may be a product dissociation step.

Transcription is a multistep process comprising enzyme−DNA interaction, initiation, processive elongation, and termination. We have examined the initiation event in transcription. Transcription initiation consists of the first and second nucleotide addition followed by the first phosphodiester bond formation, followed by a third nucleotide addition and a second phosphodiester bond formation, etc., leading to an RNA oligonucleotide of 8−12 nucleotides. Processive elongation follows the initiation process. It has been reported (*16*) that formation of the first phosphodiester bond is rate-limiting. To circumvent this step, GpG dinucleotide was used in our experiments, and therefore, the kinetic parameters reported here apply to the second phosphodiester bond formation specifically. It is likely that these parameters will also apply to the subsequent phosphodiester bond formation during the initiation process, but they may be quite different in the elongation phase. It should be possible to determine the parameters independently for the third phosphodiester bond formation using trinucleotide initiator (ref *31* and unpublished results).

Is there an effect of the rates of phosphotransfer on the processivity of the reaction? First, processivity is determined by a competition between the addition of the next nucleotide (involving PP_i release, substrate addition, and probably at least one conformational transition associated with translocation) and dissociation of the RNA oligomer. The effects of mutation on k_2 and k_{-2} tell us nothing about the rates of either of these competing processes. Second, even if k_2 and k_{-2} were relevant to processivity, we have measured these rate constants for early steps in the initiation process which has low processivity, not in the highly processive elongation process.

The burst rate constant k_{obs} for the addition of ATP to GpG by the wild-type enzyme at 21 °C is 6.1 ± 1.4 s^{-1}, whereas that for the synthesis of the trimer through hexamer using [α-^{32}P]GpG and ITP and ATP at 25 °C is 10.8 ± 1.4 s^{-1} (*16*). These values are not too different considering the differences in temperature and the system. On the other hand, the experimentally determined k_2 for the formation of GpGpA from GpG and ATP presented in this work is 3.9 s^{-1} at 21 °C for the wild-type enzyme, whereas the computer-generated rate constant for the internal nucleotide addition is 30 s^{-1} at 25 °C (*16*). Further studies are needed to formulate an overall picture of transcription initiation.

In conclusion, this study highlights the following. (i) According to pre-steady-state kinetic analysis, the mutations involving Lys → Arg and Tyr → Phe do not seem to significantly affect the intrinsic rate of phosphodiester bond formation in the initiation phase. (ii) The existence of two enzyme conformers is postulated to reconcile the differences in burst sizes between the wild type and mutants and to explain the observation that the mutant Y639F shows enzyme activity comparable to that of the wild-type enzyme when elongation is involved. In addition, possible explanations are suggested for the increase in the level of abortive initiation products generated by the mutant K631R. (iii) An interaction of Lys631 with the incoming nucleotide is suggested. (iv) The chemical step is not rate-limiting. (v) The internal equilibrium constants for the bound species are close to unity, consistent with the values for other phosphoryl transfer enzymes.

REFERENCES

1. Davanloo, P., Rosenberg, A. H., Dunn, J. J., and Studier, F. W. (1984) *Proc. Natl. Acad. Sci. U.S.A. 81*, 2035−2039.
2. Raskin, C. A., Diaz, G., Joho, K., and McAllister, W. T. (1992) *J. Mol. Biol. 228*, 506−515.
3. Li, T., Ho, H. H., Maslak, M., Schick, C., and Martin, C. T. (1996) *Biochemistry 35*, 3722−3727.
4. Osumi-Davis, P. A., de Aguilera, M. C., Woody, R. W., and Woody, A.-Y. M. (1992) *J. Mol. Biol. 226*, 37−45.

5. Osumi-Davis, P. A., Sreerama, N., Volkin, D., Middaugh, C. R., Woody, R. W., and Woody, A.-Y. M. (1994) *J. Mol. Biol. 237*, 5−19.
6. Bonner, G., Patra, D., Lafer, E. M., and Sousa, R. (1992) *EMBO J. 11*, 3767−3775.
7. Bonner, G., Lafer, E. M., and Sousa, R. (1994) *J. Biol. Chem. 269*, 25120−25128.
8. Gardner, L. P., Mooktiar, K. A., and Coleman, J. E. (1997) *Biochemistry 36*, 2908−2918.
9. Sousa, R., Chung, Y. J., Rose, J. P., and Wang, B.-C. (1993) *Nature 364*, 593−599.
10. Martin, C. T., and Coleman, J. E. (1987) *Biochemistry 26*, 2690−2696.
11. Woody, A.-Y. M., Eaton, S. S., Osumi-Davis, P. A., and Woody, R. W. (1996) *Biochemistry 35*, 144−152.
12. Beese, L. S., and Steitz, T. A. (1991) *EMBO J. 10*, 25−33.
13. Huang, Y., Eckstein, F., Padilla, R., and Sousa, R. (1997) *Biochemistry 36*, 8231−8242.
14. Ujvari, A., and Martin, C. T. (1996) *Biochemistry 35*, 14574−14582.
15. Jia, Y., Kumar, A., and Patel, S. S. (1996) *J. Biol. Chem. 271*, 30451−30458.
16. Jia, Y., and Patel, S. S. (1997) *Biochemistry 36*, 4223−4232.
17. Jia, Y., and Patel, S. S. (1997) *J. Biol. Chem. 272*, 30147−30153.
18. Grodberg, G., and Dunn, J. J. (1988) *J. Bacteriol. 170*, 1245−1253.
19. Reisbig, R. R., Woody, A.-Y. M., and Woody, R. W. (1979) *J. Biol. Chem. 254*, 11208−11217.
20. King, G. C., Martin, C. T., Pham, T. T., and Coleman, J. E. (1986) *Biochemistry 25*, 36−40.
21. Cantor, C. R., Warshaw, M. M., and Shapiro, H. (1970) *Biopolymers 9*, 1059−1077.
22. Flannery, B. P., Teukolsky, S. A., and Vetterling, W. T. (1989) *Numerical Recipes, The Art of Scientific Computing*, pp 529−538, Cambridge University Press, Cambridge, U.K.
23. Gutfreund, H. (1975) *Prog. Biophys. Mol. Biol. 29*, 161−195.
24. Gutfreund, H. (1995) *Kinetics for the Life Sciences*, Cambridge University Press, Cambridge, U.K.
25. Fersht, A. (1985) *Enzyme Structure and Mechanism*, 2nd ed., W. H. Freeman and Company, New York.
26. Johnson, K. A. (1992) *The Enzymes* (Sigman, D. S., Ed.) 3rd ed., Vol. 20, pp 2−60, Academic Press, San Diego, CA.
27. Chamberlin, M. J., and Ryan, T. (1982) *The Enzymes* (Boyer, P. D., Ed.) 3rd ed., Vol. 15, pp 87−108, Academic Press.
28. Ikeda, R. A., and Richardson, C. C. (1987) *J. Biol. Chem. 262*, 3790−3799.
29. Albery, W. J., and Knowles, J. R. (1976) *Biochemistry 15*, 5631−5640.
30. Knowles, J. R. (1980) *Annu. Rev. Biochem. 49*, 877−919.
31. Moroney, S. E., and Piccirilli, J. A. (1991) *Biochemistry 30*, 10343−10349.

BI9805801